

NUMERICAL STUDY OF EFFECT OF WALL HEATING CONDITIONS ON HEAT TRANSFER PERFORMANCE OF ROTATING INTERNAL COOLING CHANNEL

Z. Wang¹ - R. Corral^{2,1}

¹ E. T. S. de Ingenieria Aeronautica y del Espacio, Universidad Politecnica de Madrid, 28040 Madrid, Spain

Email: zhi.wang@upm.es

² Advanced Engineering Direction, Industria de TurboPropulsores S.A., 28108 Alcobendas, Spain

Email: roque.corral@itp.es

ABSTRACT

This paper investigates the impacts of wall heating conditions on heat transfer performance for a rotating channel with one side smooth and one side roughened by 45 degree inclined ribs. Previous experimental and numerical studies for only ribbed wall heated case showed that rotation has significantly negative impact on heat transfer performance. In order to investigate this uncommon behaviour, RANS simulations were conducted under three different wall heating conditions in present study: ribbed wall heated, all walls heated and adiabatic conditions. Numerical results show that the uneven wall heating conditions has negligible impact on stationary case, however, it has a large influence on rotational cases, in both the heat transfer and the fluid field. This is because in rotating cases, uneven heatings result in different buoyancy effects on trailing and leading walls that alter the main flow velocity profile. As a consequence, also secondary flows and heat transfer performance are affected.

NOMENCLATURE

AR	Aspect ratio	Pr	Prandtl number
Bo	Buoyancy number	Re	Reynolds number
d_h	hydraulic diameter	Ro	Rotational number
e	rib height	T_{ref}	Reference temperature
e/d_h	blockage ratio	T_w	wall temperature
Nu	Nusselt Number	Nu_0	Dittus-Boelter correlation (heating)
U_0	Inlet mean velocity	U_x	Stream-wise velocity
U_y	Span-wise velocity		

INTRODUCTION

The continuous efforts for improving efficiency and thermal performance in modern aero-engines lead to the use of very high turbine entry temperatures and to minimise the amount of coolant flow consumption. Therefore, highly sophisticated cooling techniques are essential to maintain gas turbine safety and durability under such extreme conditions. In order to increase

the heat transfer performance of internal cooling systems, complex internal cooling channels are cast in the blades, enhanced by using artificial roughness elements or turbulence promoters such as ribs, pin-fins or dimples.

There are many parameters affect the performance of rib-roughened channels. For instance, the aspect ratio and orientation of the channel, as it can vary within a wide range depending on the location of the channels inside the turbine blade. The influence has been discussed by Han (1988); Dutta and Han (1996). Rib installation inside the channel, such as the orientation, spacing, or blockage ratio also have significant impacts on the flow passing through the channel and therefore, the heat transfer enhancement. Besides, since turbine rotor blades rotate at very high rotation speed, the coolant flow passing through internal channels experiences two additional forces: Coriolis forces and centrifugal buoyancy forces. These forces induce secondary flows and vortexes in transverse direction along the channel resulting in very complex flow-fields. In a ribbed channel, Coriolis forces interact with the separated flow promoted by a variety of turbulent devices producing a large diversity of secondary flows, that characterise their corresponding heat transfer performance. As a result, the interaction of the secondary flow induced by rotation, and the rib turbulators results in heat transfer patterns different from stationary channels. According to a considerable amount literature, the understanding is that, the rotational effects will enhance heat transfer performance on pressure side, whereas it will reduce it on suction side in an orthogonal rotating channel Griffith et al. (2002a); ?. These geometrical and rotational effects been devoted to evaluating heat transfer characteristics in a vast number of experimental and numerical investigations over passed 40 years. Overall reviews of the background and advances in this field can be found in Han and Chen (2006) and Ligrani (2013).

Additionally, wall heating conditions may also have impact on heat transfer performance in rotating channels. In real turbine rotor blades, due to the characteristics of main annulus flow, pressure side and suction side of turbine blade experience different thermal loads. Therefore, this uneven wall heating effect has to be considered in the design process to minimise thermal stress. In addition, in experimental setups, it is common to heat only one wall when optical access is involved Coletti et al. (2014); Mayo, Lahalle, Gori and Arts (2016) due to measurement considerations. An in-depth discussion of this kind of set-up can be found in Coletti et al. (2014).

It appears that not many researches have addressed this issue, only little literature Han and Zhang (1992); Parsons et al. (1994); Zhang et al. (1995); Hsieh and Liu (1996) on the effect of heating one or more of the channel walls at different levels exists. It was found that the actual impact on heat transfer level was significant. They presumed that the impact was due to the Coriolis-induced cross stream secondary flows, which altered the local coolant temperature by carrying hotter or cooler fluid towards the leading or trailing wall. However, there is a lack of discussion in the references. This uneven heating condition also creates an unbalanced buoyancy force at the leading and trailing walls, which in turn may alter the flow as well as the heat transfer behaviour when rotating at high Buoyancy numbers. Because of the difficulties associated with simultaneous flow and heat transfer measurements, it is still unclear if the changes of the heat transfer are also due to the alteration of the flow-field. Therefore, it is necessary to systematically study this complex flow and heat transfer behaviour with the help of numerical methods.

The objective of present paper is to numerically investigate the impact of uneven wall heating conditions on the internal flow and heat transfer performance of a 45° rib roughened rotating

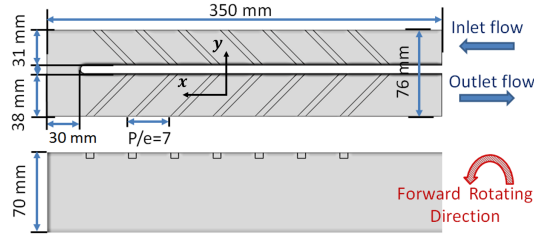


Figure 1: Cooling Channel Sketch

channel. Our earlier study with only one wall heated case showed reasonable agreement against experimental data (Wang et al., 2016). However, an uncommon behaviour was consistently observed by both, numerical simulation and experiment data. The heat transfer on trailing wall was reversely affected by rotation in a radially outward flow channel. We suspect that uneven heating may play an important role, since most of studies associated with 45° inclined rib channels consider that all the walls are heated.

ROTATING CHANNEL MODEL

The testing geometry was designed by SNECMA based on a real HPT rotor blade two-pass internal cooling channel. It consists of two rectangular channels connected by a 180° sharp turn. The overall dimensions of the test channel can be found in Fig. 1. The total length of the channel is 350 mm, and the height 70 mm. The width of the upstream and downstream passages is 31 mm and 38 mm, respectively. The web thickness between the two channels is 7 mm and the distance between the divider wall and outer end wall is 30 mm. The outward upstream passage has an aspect ratio of $AR = 1 : 2.25$ and after the turn, the inward downstream passage has an aspect ratio $AR = 1 : 1.85$. One side of the two channels is equipped with 45° square cross section skewed rib turbulators, with a rib spacing $P/e = 6$ and a blockage ratio $e/d_h = 0.116$, where the hydraulic diameter is referred to the upstream passage. In total 14 ribs are arranged in parallel, while the other side remains smooth in order to ease the optical access in experiment. Details of experimental set-ups can be found in Wang et al. (2016).

NUMERICAL SET-UP

Previous studies (Wright et al., 2005a; Huh et al., 2011) have shown that, the entry shape can have a significant impact on the flow-field and heat transfer performance. Therefore, the computational domain was extended to include the supply system in order to account for inlet entry effects. Figure 2 shows the computational domain and mesh used in the numerical simulations. The inlet/outlet supply system has a circular pipe shape that transitions to a C-shaped pipe near the joint with the transition pipe to create an engine-similar entry flow. The model is discretised by means of unstructured hybrid grids using an in-house mesh generator. The grid consists of a near-wall prismatic layer region, while the rest of the domain is discretised using isotropic tetrahedral elements. In total, 18 prismatic layers are constructed with $y^+ < 1$ for all the tested Reynolds numbers. The total grid size is 13.5 million cells. A sensitivity study was performed with a 8 million cell model, and the change in the section averaged heat transfer coefficient was less than 3%. Hence, the solution obtained in current study is considered grid independent

Steady-state simulations have been conducted using in-house RANS code Mu^2s^2T , Burgos

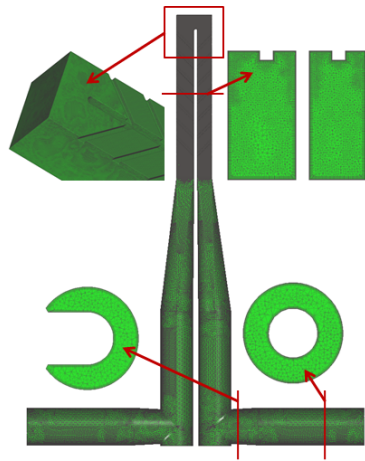


Figure 2: Hybrid Mesh of Computational Domain

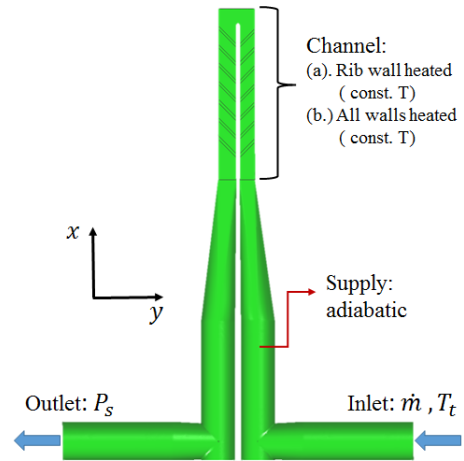


Figure 3: CFD Boundary Condition Set-up

et al. (2011). The code solves the 3D RANS equations using an edge-based data structure to spatially discretise the equations using a MUSCL scheme. Low Mach preconditioning is used to enhance the convergence and accuracy for low Mach number flows. The code is fully parallelised using MPI and executed on GPUs to improve computational efficiency.

The turbulence effects were accounted for using the $k - \omega$ SST turbulence model (Menter, 1994) with an inlet turbulence intensity of 5%. The inlet/outlet boundary conditions have been obtained from experimental measurements. Temperature and mass flow rate are provided at the inlet, and static pressure is set at outlet. This numerical study was performed at Reynolds number $Re=15,000$ under three rotating conditions: stationary ($Ro = 0$); forward rotation direction ($Ro = 0.3$), where the ribbed surface behaves as the trailing wall (pressure side) of a rotor blade; and backward rotation direction ($Ro = -0.3$), where the ribbed surface behaves as leading wall (suction side).

In order to investigate the effect of wall heating conditions. Three wall boundary conditions were tested: (a). Only ribbed wall heated, (b). All walls heated, (c). Adiabatic. The mean Buoyancy number, Bo is about 0.17 in Case (a) and (b), as in experiment. While the supply system is set as adiabatic in all cases. The overall boundary conditions can be found in Fig. 3.

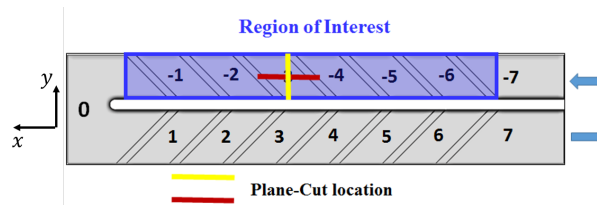


Figure 4: Segment index notation

RESULTS

For the sake of clarity, hereby we only consider the wall heating effect in the first pass where rotating Coriolis and buoyancy effects are more conspicuous. For flow domain investigation, we take the segment No. -3 of the first pass, since it is away from the influence of the bend and entrance. The region of interest and segment notation is illustrated in Fig. 4

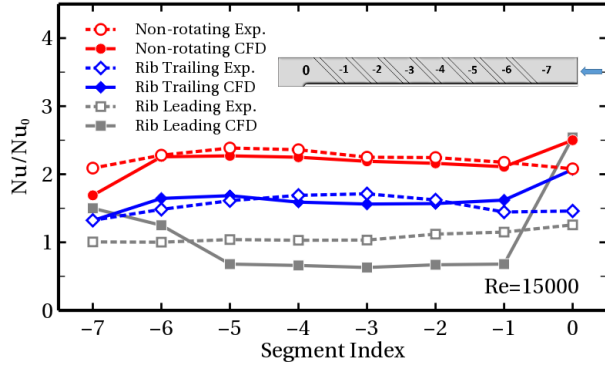


Figure 5: Normalised Segment Averaged Nusselt Number: EXP-CFD

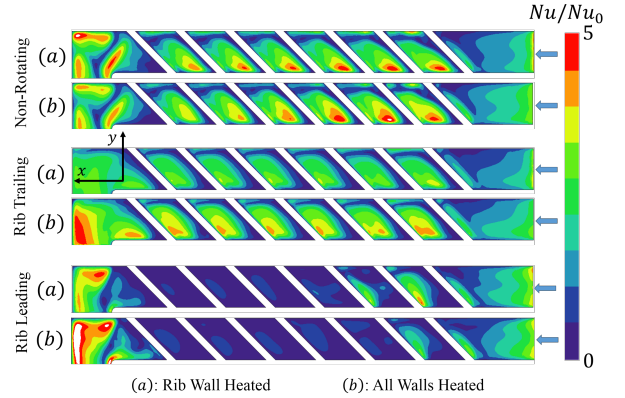


Figure 6: Numerical results of Nu/Nu_0 distribution for different wall heating conditions

Segment Averaged Heat Transfer Validation

In order to validate the numerical results, the normalised segment averaged Nusselt number based on the smooth area between ribs is presented. The Nusselt number is normalised with the Dittus-Boelter correlation (Kays et al., 2012).

$$Nu_0 = 0.023Re^{0.8}Pr^{0.4}$$

Figure 5 shows the comparison between experimental and numerical results with only the ribbed wall heated case (Case (a)) in the first passage. It can be seen that, the segment averaged heat transfer data in non-rotating and ribbed surface rotating as trailing wall case (Rib-TR) are well predicted. For the ribbed surface acting as leading wall, case (Rib-LE), the numerical results over-predict the negative effect of rotation, underestimating the heat transfer in overall by about 30%-35% when compared with the experimental data. Because rotation stabilises the flow at the leading wall and enlarges the separation zone, especially when the wall is heated (Coletti et al., 2014). The flow in this case is fully separated causing difficulties to the turbulence model to accurately predicts the heat transfer rate, since the commonly used turbulence models are not designed to account for the turbulent fluctuations generated inside a recirculation bubble. A turbulence model behaves as a laminar case inside a large separation bubble and the computed heat transfer in this region is correspondingly lower since the physical existing fluctuations are disregarded in practise. However the heat transfer decrease due to the separation is qualitatively predicted.

The most interesting result is that, on the contrary than in previous works (Huh et al., 2011), the heat transfer efficiency drops, in the ribbed trailing wall (Rib-TR) case, compared to stationary case. This behaviour is consistent, both in the experiments and in the numerical simulations. Moreover the magnitude of the drop in the upstream passage of Rib-TR case, is large, being about 25%. This variation is much larger than the uncertainties that could be reasonably associated to either the experimental or numerical techniques used in here.

Wall Heating Effect on Heat Transfer Distribution

Figure 6 shows the contour plots of the normalised Nusselt number distributions obtained from the numerical simulations for different heating conditions. In the absence of rotation, it is

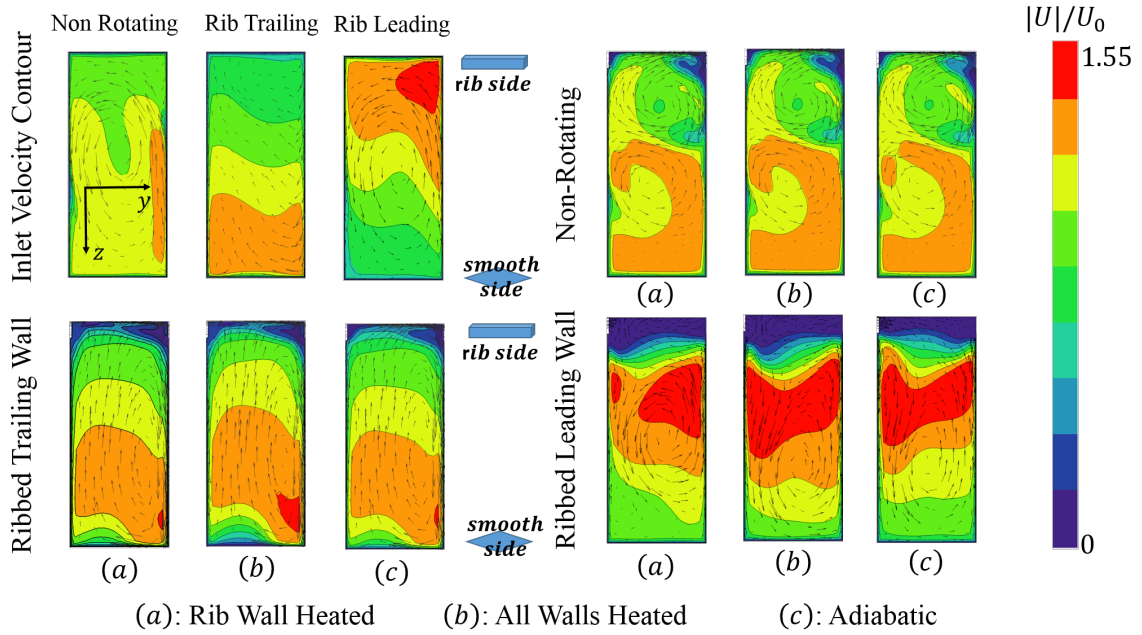


Figure 7: Velocity and secondary flow features at channel inlet and at middle of segment no. -3 for different wall heating conditions

shown that cases (a) and (b) only have tiny variations in heat transfer level, indicating that the flow field is essentially the same for different wall heating conditions.

For the ribbed trailing rotating test, case (b) has a significantly higher heat transfer at the wall than case (a). The overall patterns are similar, but the peak regions in case (b) has enlarged and displaced slightly upstream compared to case (a). This suggests that the main flow features in the vicinity of the ribbed wall have not substantially changed. However, the flow reattachment behaviour and the absolute level may have been modified and should be further investigated.

In the ribbed leading rotating test, very low heat transfer rates are observed in both cases. Therefore, it can be conjectured that large recirculation bubble may dominate the inter-rib regions in both cases. However it is not possible to deduce the detailed flow behaviour from this heat transfer pattern since this is quite low.

Secondary Flow Characteristics

In order to enhance the understanding and further analysis of this complex flow-field, The secondary flows and velocity patterns are presented. Figure 7 displays the relative velocity contours and secondary flow features at the channel inlet, and at the middle of segment No. -3 (yellow line of Fig. 4). The relative velocity is normalised with the mean inlet velocity, U_0 . The inlet velocity contours show that the entry geometry formed a counter clock-wise secondary flow at the middle of the channel in the non-rotating case. This secondary flow is weakened in rib trailing wall case, whereas it is preserved in rib leading wall case due to the interaction with Coriolis induced secondary flow. It is clearly seen that, under the action of rotation, the inlet velocity profiles are significantly altered with respect to the non-rotating case. However, the entry flow profiles are identical for all the heating conditions, since there is no heating in the air supply system. Thus, it will not be shown repeatedly.

In the non-rotating tests, the presence of inclined ribs (upper side) induces a high momentum

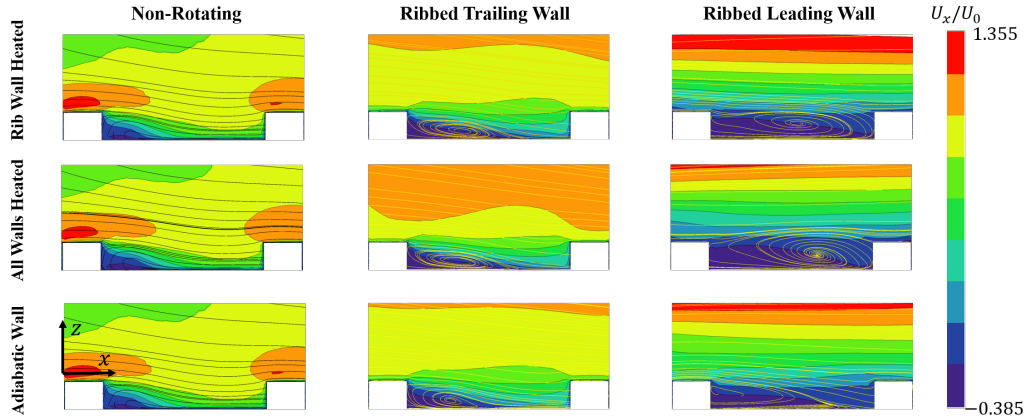


Figure 8: Stream-wise velocity contours and streamlines in inter-rib region for different wall heating conditions

span-wise flow along the rib creating a strong clockwise vortex in the vicinity of the ribbed wall regions. Unlike the straight rib channel, in which the heat transfer is mainly dependent on the separation-reattaching stream-wise flow, this span-wise motion strongly affects the heat transfer behaviour by aggressively increasing the flow velocity, and bringing cooler fluid to the rib wall Viswanathan and Tafti (2006). Meanwhile, the entry shape formed counter clockwise vortex is pushed to the lower part of the channel. It is observed that the flow field in this case remains unchanged for different wall heating conditions, because of the heat is effectively convected downstream in this case.

In the ribbed trailing wall tests, rotation induces a secondary flow which moves fluid from the leading surface (bottom) to the trailing surface (top) of the channel. At the side wall, where the fluid is moving slow, the pressure gradient creates flow with the opposite sense, from upper side to lower side, to close the vortex. Figure 7 shows that the secondary flow patterns are essentially the same, however there are significant changes in the velocity field. Compared to the rib wall heated case (case (a)), the velocity is skewed towards the upper ribbed trailing wall when all the walls are heated (case (b)), therefore a higher velocity is observed in the vicinity of the ribbed wall regions. In addition, a reduced velocity appears at the leading wall in case (b) compared to cases (a) and (c). The underlying reason is that when a wall is heated, near wall regions have lower density than the mean flow due to the temperature variation. Therefore, the Buoyancy force acts in opposite direction to the stream-wise flow. As a result, this hotter flow will be slowed down, and the cooler flow will be accelerated to keep mass continuity. This can be clearly seen at leading wall in case (b), compared to cases (a) and (c).

In the ribbed leading wall tests, very low velocity regions appears in the vicinity of ribbed wall (see Fig. 7), suggesting that the heat transfer level is much lower than in the non-rotating and ribbed trailing wall tests. The secondary flow shows similar patterns for different wall heating conditions, moving fluid from the leading side to trailing side and back to leading side along the side wall. The presence of the central vortex is due to the interaction of secondary flow induced by the Coriolis force and the entry shape.

The ribbed leading wall case exhibits the opposite behaviour compared to ribbed trailing wall due to the change of the rotating direction. The velocity profile in the all wall heated case (case (b)) was displaced towards the bottom (smooth trailing surface) under the same effect of

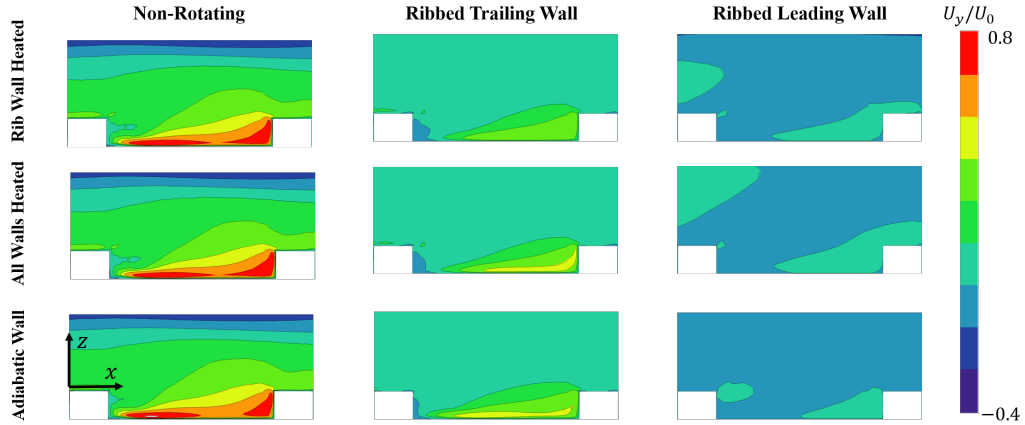


Figure 9: Span-wise velocity contours in inter-rib region for different wall heating conditions

the Buoyancy force analysed above.

Inter-Rib Flow Characteristics

The impact of wall heating conditions in the vicinity of ribbed wall can be investigated by analysing inter-rib flow field. Figures 8 and 9 display the stream-wise and span-wise velocities at the inter-rib region for different wall heating conditions at the middle of segment No. -3 (red line in Fig. 4). The main characteristics of the flow in the non-rotating channel is that, the flow accelerates on the top of the rib due to the blockage of the cross section area, then a sudden expansion and the creation of a recirculation bubble with low momentum fluid are created. The recirculation bubble height is reduced due to the mixing with high momentum fluid of the core near the rib region. In addition, it is worth to notice that, in the non-rotating tests, the magnitude of span-wise velocity induced by the inclined ribs is very high. It induces mixing that in turn promotes a faster re-attachment in the inter-rib recirculation region, and therefore, high heat transfer can be expected. Similarly as analysed in the previous subsection, wall heating conditions have very little impact on the flow-field in the non-rotating case.

In the ribbed trailing wall tests, it can be observed that different heating conditions alter the flow-field more significantly. In the adiabatic case, the recirculation bubble re-attaches faster than in the two heated cases (see Fig. 8(middle)). The re-attaching was contributed by the destabilising effect of rotation, which enhances the entrainment of fluid from the recirculation bubble to the main flow, as well as the magnitude of rib induced span-wise flow. However, because of the Coriolis induced and rib induced secondary flow are acting in the opposite direction, the interaction reduces the magnitude of span-wise flow (see Fig. 9) compared to that of the non-rotating tests, resulting in a larger separation area.

When the ribbed wall is heated, the adjacent fluid experiences a centripetal buoyancy force in the upstream direction. This phenomenon can be explained using the schematic model shown in Fig. 10. Because of the heating, the recirculation region behind the rib has a higher temperature than the core flow, therefore the rotating buoyancy force acts in the opposite direction of the stream-wise flow. Thus, the recirculation area is slightly enlarged in the two heated cases compared to the adiabatic case. However, when all walls are under heating, due to the fact that leading wall has a lower heat transfer rate than the trailing wall, the fluid is hotter and the density lower than in the mainstream. As a result, the flow near the leading wall experiences a higher

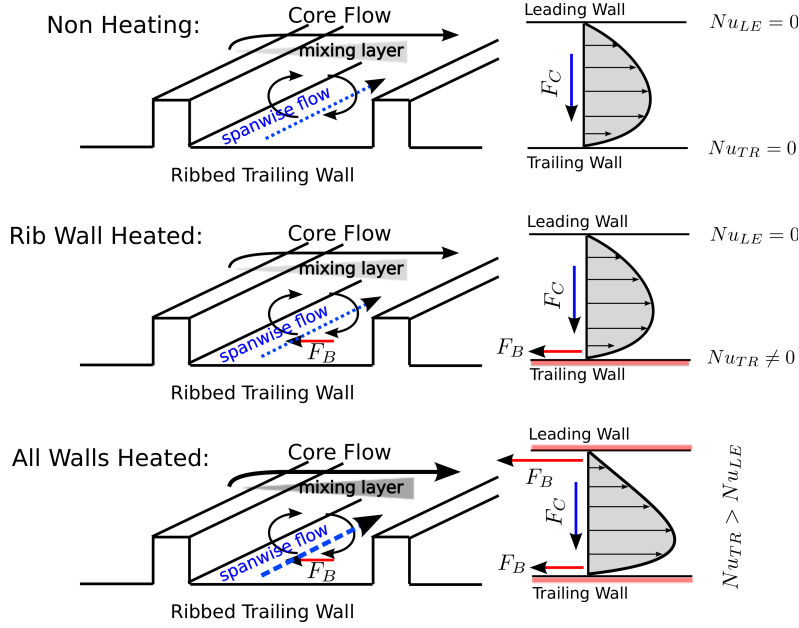


Figure 10: Schematic Model of flow in ribbed trailing wall tests, under Coriolis and buoyancy forces

buoyancy force than the trailing wall. By the contribution of unbalanced buoyancy forces, the flow velocity near leading surface is slowed down and pushed toward to the trailing surface. This flow motion enhances the mixing with the separation bubble by increasing the momentum of near wall fluid and the Coriolis effect. As a consequence, the size of recirculation bubble in the all wall heated case is slightly reduced compared to that of the ribbed wall heated case. Therefore, higher heat transfer can be expected.

When the ribbed wall behaves as leading wall, the shear layer generated by the rib is stabilised by the rotation and the entrainment of fluid from the separation bubble to the main stream is strongly reduced, resulting in an much larger recirculation area. When ribbed wall is heated, the recirculation bubble is further enlarged by buoyancy forces in both stream-wise and wall normal directions that occupies the whole inter-rib regions. Very low momentum fluid in both the stream-wise and span-wise directions leads to a very low heat transfer as shown in Fig. 6.

Overall Flow Field and Heat Transfer Characteristics

The stream-wise velocity profile along the channel height is presented in Fig. 11. The channel height is normalised with the height of the rib. It can be seen that due to the entry shape and the asymmetry of the channel, the stream-wise velocity in non-rotating tests does not show a typical channel flow profile. But once again it confirms that wall heating conditions do not alter the overall flow field in non-rotating case.

In the ribbed trailing tests, Fig. 11 (middle) shows the enlarged separation bubble size from the two heated cases to adiabatic case, as explained in previous subsection. The stream-wise flow near the leading surface (top) in the all walls heated case is strongly reduced, and the fluid core is pushed towards to the ribbed trailing wall (bottom). Also, the comparison between rib wall heated case and adiabatic case suggests that the variation of stream-wise velocity is local and the overall flow field is almost unaffected when only the trailing wall is heated.

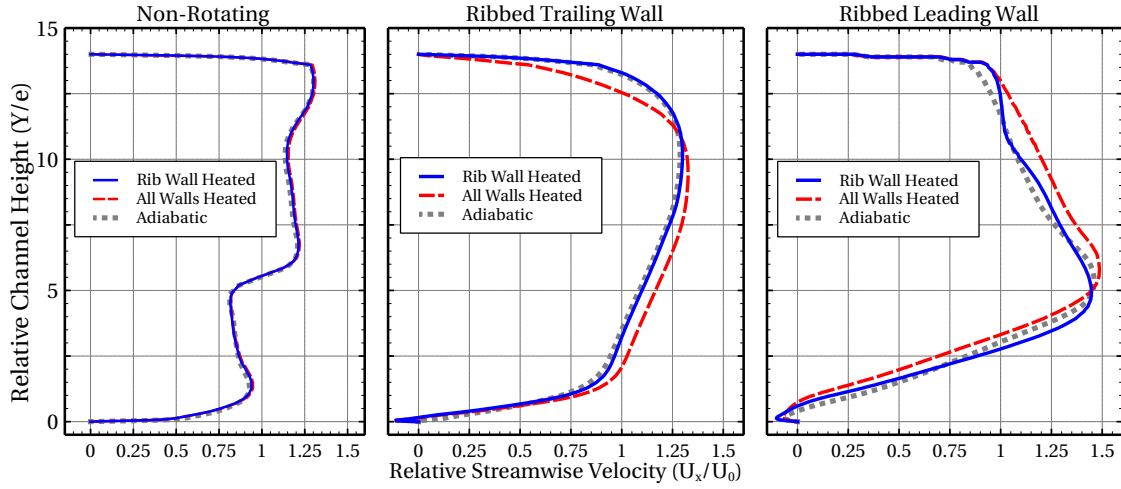


Figure 11: Stream-wise velocity profile along channel height at middle plane of segment -3 for different wall heating conditions

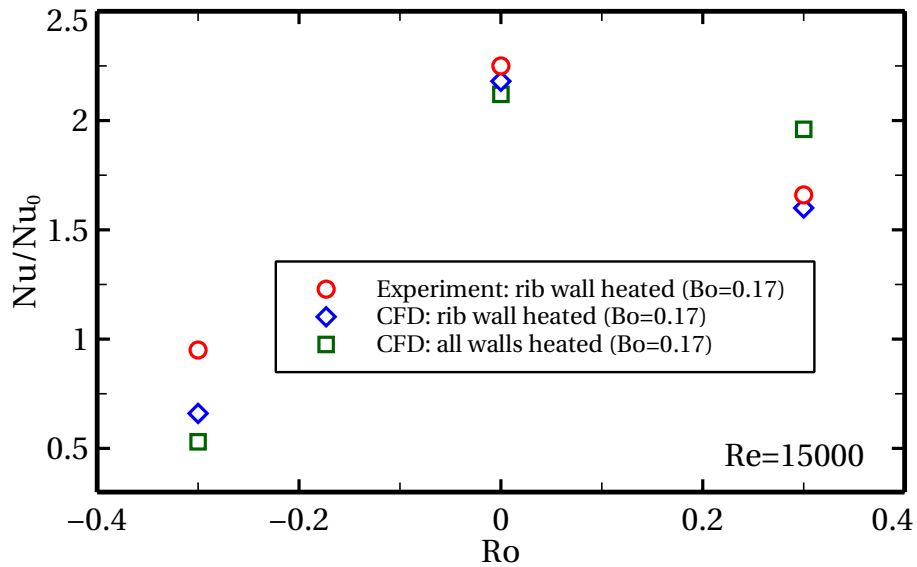


Figure 12: Overall normalised Nusselt number for different wall heating conditions: EXP vs CFD

In the ribbed leading wall tests, Fig. 11 shows a displacement of fluid towards the trailing side (top) in the all walls heated case due to the presence of buoyancy force. In addition, the flow in the vicinity of the trailing wall (top) shows similar contours under the three heating conditions, confirming the finding that the impact of the buoyancy is smaller in the trailing wall than in the leading wall.

In the end, the overall heat transfer performance of the entire first passage is summarised in Fig. 12. It is shown that in the ribbed trailing wall tests, the heat transfer level is significantly higher in all wall heated case than in only rib wall heated case. The value is more close to the non-rotating case as described in Viswanathan and Tafti Viswanathan and Tafti (2006). The flow domain investigation confirms that this variation is mainly due to the centripetal buoyancy effect that alters the flow profile inside the channel by reducing the velocity at leading wall and

pushing the fluid core towards the trailing wall. This behaviour enhances the heat transfer by bringing cold, high momentum fluid, as well as increasing the strength of Coriolis effect in the vicinity of ribbed trailing wall. In the ribbed leading wall tests, the overall heat transfer rate is slightly lower in all walls heated case than in only rib wall heated case. This is possibly because in the ribbed leading wall case, the secondary flow also brings hot fluid back to the leading surface along side walls, therefore increasing the local temperature and enlarging the buoyancy effect. However, since the heat transfer level is low, the variation is not as significant as in trailing wall tests.

CONCLUSIONS

This paper investigates the impact of the wall heating conditions on flow and heat transfer performance of a rotating channel with one side smooth and one side roughened by 45 degree inclined ribs. RANS simulations were conducted under three different wall heating conditions in the present study: ribbed wall heated, all walls heated and adiabatic conditions. Numerical results has shown that uneven wall heating conditions have negligible impact on the non-rotating case. However, large impacts, both in the heat transfer and flow field can be seen under rotation. The heat transfer level is significantly higher in the all wall heated case than in the only ribbed wall heated case, when the ribbed wall acts as the trailing surface, and slightly reduced when the ribbed wall is in the leading surface.

The flow-field investigation shows that this variation is mainly due to rotating buoyancy effect. In rotating cases, uneven heating induces different buoyancy effects on the trailing and the leading walls, that alter the velocity profile of the main flow. As a consequence, also secondary flows and heat transfer performance are affected. When only one wall is heated, the buoyancy only alters the flow in the vicinity of heated wall, and the trailing surface is significantly less affected than the leading surface.

According to the results obtained in the paper, we conclude that when buoyancy effects are relevant. The heating settings can play a significant role in the heat transfer mechanisms and therefore in the experimental and numerical results.

ACKNOWLEDGEMENTS

The research leading to these results has received funding from the European Union Seventh Framework Programme (FP7/2007-2013) under grant agreement No. 233799 (ERICKA). The authors wish to thank Industria de Turbopropulsores S.A. (ITP) for its technical support and computing resource. The ERICKA consortium and members, in particular ITP, ONERA, and SNECMA, are greatly acknowledged for allowing the authors to publish this paper.

REFERENCES

- Burgos, M. A., Contreras, J. and Corral, R. (2011). Efficient edge-based rotor/stator interaction method, *AIAA journal* **49**(1): 19–31.
- Coletti, F., Jacono, D. L., Cresci, I. and Arts, T. (2014). Turbulent flow in rib-roughened channel under the effect of coriolis and rotational buoyancy forces, *Physics of Fluids* **26**(4): 045111.
- Dutta, S. and Han, J.-C. (1996). Local heat transfer in rotating smooth and ribbed two-pass square channels with three channel orientations, *Journal of Heat Transfer* **118**(3): 578–584.

- Griffith, T. S., Al-Hadhrami, L. and Han, J.-C. (2002a). Heat transfer in rotating rectangular cooling channels ($ar=4$) with angled ribs, *Journal of Heat Transfer* **124**(4): 617–625.
- Han, J. (1988). Heat transfer and friction characteristics in rectangular channels with rib turbulators, *Journal of Heat Transfer* **1**: 321–328.
- Han, J.-C. and Chen, H.-C. (2006). Turbine blade internal cooling passages with rib turbulators, *Journal of Propulsion and Power* **22**(2): 226–248.
- Han, J.-C. and Zhang, Y. (1992). Effect of uneven wall temperature on local heat transfer in a rotating square channel with smooth walls and radial outward flow, *Journal of heat transfer* **114**(4): 850–858.
- Hsieh, S.-S. and Liu, W.-J. (1996). Uneven wall heat flux effect on local heat transfer in rotating two-pass channels with two opposite ribbed walls, *Journal of heat transfer* **118**(4): 864–876.
- Huh, M., Lei, J., Liu, Y.-H. and Han, J.-C. (2011). High rotation number effects on heat transfer in a rectangular ($ar=2:1$) two-pass channel, *Journal of Turbomachinery* **133**(2): 021001.
- Kays, W. M., Crawford, M. E. and Weigand, B. (2012). *Convective heat and mass transfer*, Tata McGraw-Hill Education.
- Ligrani, P. (2013). Heat transfer augmentation technologies for internal cooling of turbine components of gas turbine engines, *International Journal of Rotating Machinery* .
- Mayo, I., Lahalle, A., Gori, G. L. and Arts, T. (2016). Aerothermal characterization of a rotating ribbed channel at engine representative conditions-part ii: Detailed liquid crystal thermography measurements, *Journal of Turbomachinery* **138**(10): 101009.
- Menter, F. R. (1994). Two-equation eddy-viscosity turbulence models for engineering applications, *AIAA journal* **32**(8): 1598–1605.
- Parsons, J. A., Je-Chin, H. and Yuming, Z. (1994). Wall heating effect on local heat transfer in a rotating two-pass square channel with 90 rib turbulators, *International Journal of Heat and Mass Transfer* **37**(9): 1411–1420.
- Viswanathan, A. K. and Tafti, D. K. (2006). Large eddy simulation of fully developed flow and heat transfer in a rotating duct with 45 degree ribs, *ASME Turbo Expo*, American Society of Mechanical Engineers, pp. GT2006–90229.
- Wang, Z., Corral, R. and Chedevergne, F. (2016). Experimental and numerical study of heat transfer performance for an engine representative two-pass rotating internal cooling channel, *ASME Turbo Expo*, American Society of Mechanical Engineers, pp. GT2016–57419.
- Wright, L. M., Fu, W.-L. and Han, J.-C. (2005a). Influence of entrance geometry on heat transfer in rotating rectangular cooling channels ($ar=4:1$) with angled ribs, *Journal of Heat Transfer* **127**(4): 378–387.
- Zhang, Y., Han, J., Parsons, J. and Lee, C. (1995). Surface heating effect on local heat transfer in a rotating two-pass square channel with 60 deg angled rib turbulators, *Journal of turbomachinery* **117**(2): 272–280.